

A W-Band Integrated Power Module Using MMIC MESFET Power Amplifiers and Varactor Doublers

Thomas C. Ho, *Senior Member, IEEE*, Seng-Woon Chen, Krishna Pande, *Fellow, IEEE*, and Paul D. Rice

Abstract—A high-performance integrated power module using *U*-band MMIC MESFET power amplifiers in conjunction with *W*-band MMIC high efficiency varactor doublers has been developed for millimeter-wave system applications. This paper presents the design, fabrication, and performance of this *W*-band integrated power module. Measured results of the complete integrated power module show an output power of 90 mW with an overall associated gain of 29.5 dB at 94 GHz. A saturated power of over 95 mW was also achieved. These results represent the highest reported power and gain at *W*-band using MESFET and varactor frequency doubling technologies. This integrated power module is suitable for the future 94 GHz missile seeker applications.

I. INTRODUCTION

THE next generation millimeter-wave systems require high-performance, reliable, and low-cost monolithic solid-state components to be affordable. Monolithic millimeter-wave integrated circuits (MMIC's) offer the greater potential to reduce cost, enhance performance, and improve the reliability of such systems. Considerable effort is, therefore, being directed toward the development of monolithic millimeter-wave integrated circuit components for radar, missile seeker, communications, smart weapon, electronic warfare, and radiometry system applications. The 94 GHz monolithic power transmitters have potential application for *W*-band missile seekers and phased array radars. However, no such transmitters are readily available due to the lack of power amplifiers with desired output power of 80 mW at 94 GHz. Although pseudomorphic InGaAs and lattice matched InP high-electron mobility transistors (PHEMT) with multiquantum well structures show excellent potential for power amplification at *W*-band [1]–[3], their usage is limited due to relatively low yield as a result of 0.1- μ m gate lengths. Moreover, their reliability has yet to be established for power amplification. Therefore, the option of doubling 47 GHz of output power to 94 GHz is quite attractive, since reliable high yield 0.3 μ m gate length FET's [4] can be used for the 47 GHz power amplifier chips.

In this paper, we present the design, fabrication, and performance of a state-of-the-art *W*-band integrated power module, using a 0.6-watt *U*-band power MESFET MMIC amplifier in conjunction with *W*-band high efficiency MMIC varactor doublers, to generate 95 mW transmitted power at *W*-band. Measured results of the complete integrated power module show an output of 90 mW with an overall associated gain of 29.5 dB at 94 GHz. A saturated output power of 95 mW was also achieved. These results represent the highest power and gain at *W*-band using MESFET and varactor frequency doubling technologies. The developed four-way combined MMIC power amplifier demonstrated 460 mW output power with an associated gain of 16.6 dB at 47 GHz. The saturated output power of this amplifier exceeded 580 mW. The doubler chip uses a 16- μ m diameter Schottky contact varactor that has a buried n^+ layer and has exhibited a state-of-the-art performance, maximum efficiency of 25% (6 dB conversion loss), and output power of 55 mW at 94 GHz. A saturated output power of 65 mW was also obtained at the same frequency. This integrated power module can reliably produce greater than 90 mW of output power at 94 GHz as a transmitter source for missile seeker applications.

The configuration of integrated power modules will be described in Section II. The MMIC circuit design and fabrication are presented in Sections II and III, respectively. Section IV, summarizes the circuit performance and Section V is the conclusion.

II. CIRCUIT DESIGN

Fig. 1 shows a block diagram of the 47–94 GHz integrated power module. The developed integrated power module is composed of a four-stage MMIC power amplifier, a four-way combined 0.6-watt 47-GHz power amplifier, and two-way combined 94 GHz MMIC doublers using off-chip Wilkinson type divider/combiner circuits. Based on this approach, the state-of-the-art output power of 95 mW, with about 28 dB associated gain at 94 GHz, has been achieved.

U-Band Power Amplifier

A high performance four-stage 47 GHz monolithic power amplifier was developed using a 400- μ m gate width

Manuscript received March 22, 1993; revised June 7, 1993.

T. C. Ho, S. W. Chen, and K. Pande are with COMSAT Laboratories, Clarksburg, MD 20871.

P. G. Rice is with Hercules Defense Electronics Systems, Inc., Clearwater, FL 34618.

IEEE Log Number 9212998.

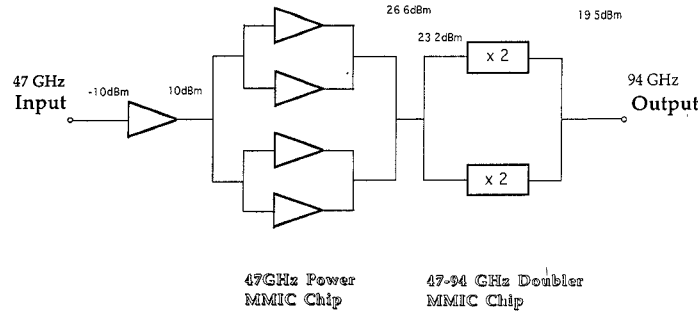
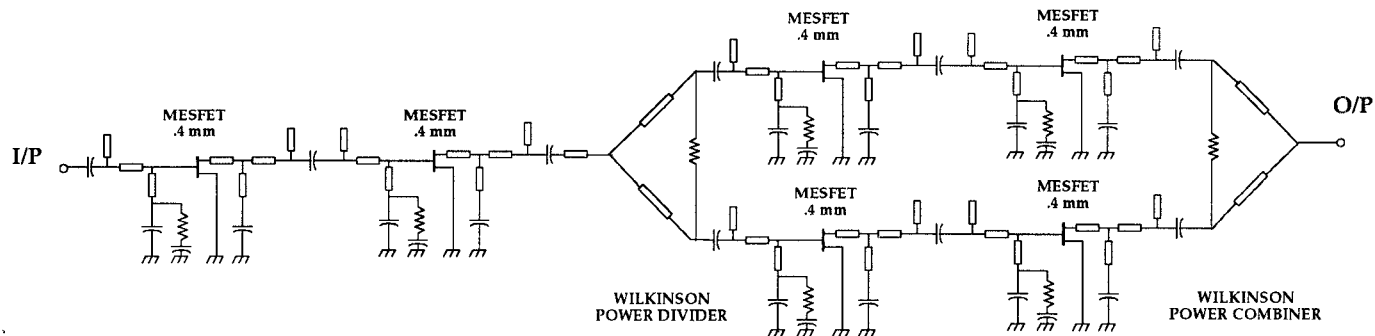
Fig. 1. Block diagram of *W*-band integrated power module.

Fig. 2. Circuit schematic of four-stage MMIC power amplifier chip.

MESFET device. The amplifier design consists of a two-stage driver amplifier followed by a two-stage power amplifier. Fig. 2 shows the circuit schematic of the four-stage MMIC power amplifier chip. The baseline monolithic driver amplifier design consists of a two-stage, 400- μ m MESFET amplifier. The power stage consists of a pair of two-stage driver amplifiers combined using integrated in-phase Wilkinson-type divider/combiner circuits. A high-frequency small-signal equivalent circuit was obtained for the MESFET device by matching an equivalent circuit model to the measured *S*-parameters up to 40 GHz. The optimal load impedance, required by the MESFET device to deliver its maximum power at 47 GHz, was calculated with a load-pull simulation program [5] [6]. Both the equivalent circuit model and optimal load impedances were used for the MMIC power amplifier design. In the MMIC circuit design, the output matching circuit was designed for optimal load impedance to the MESFET in its bandwidth of operation, resulting in maximum delivered power in that bandwidth. The input matching circuit was designed for a conjugate match to the MESFET input impedance with the device terminated with the optimal load impedance to achieve maximum power gain. The input match was then optimized for input return loss and gain flatness across the design bandwidth by using Touchstone microwave circuit analysis program. The stabilizing RC circuits were integrated with the gate bias networks to ensure unconditional stability of the chip operation down to few megahertz region. A resistor/divider circuit was also included to bias FET gates of each amplifier stage at a nominal value of -0.7 V with a power supply of -5 V. At the drain side, the +5 V power supply voltage

of the system was applied to each amplifier stage directly, without scaling to bias the drain.

To achieve usable power and gain for system applications, a four-way combined power amplifier using the above four-stage power MMIC chips was also developed. The hybrid combiners and dividers were regular in-phase and 90° offset Wilkinson-type circuits to form a four-way combining circuit. This four-way combiner/divider was fabricated on 5-mil-thick fused silica substrate. Four power MMIC chips, together with a four-way combiner/divider, were mounted on a flat center block as shown in Fig. 3. The amplifier block was then sandwiched between two ridged waveguide-to-microstrip transitions.

W-Band Varactor Doubler

Successful development of a doubler circuit hinges on proper design and accurate modeling of the varactor diode. Assuming the current density is confined parabolically within a skin depth δ , the series resistance R_s , including spreading resistance and skin effect, can be derived based on previous work [7], [8]. The diode junction capacitance C_j and the breakdown voltage V_B can also be estimated accurately [9]. The doubling efficiency η and maximum output power, P_{out} , of an abrupt junction varactor diode can be predicted from R_s , C_j , and V_B [10], [11]. Variation of a varactor diode series resistance and cut-off frequency with the active layer doping concentration has been analyzed and simulated. Based on the results of the optimization, a varactor diode with a 16- μ m diameter Schottky contact and an active layer of $7 \times 10^{16} \text{ cm}^{-3}$ doping concentration were chosen for optimum efficiency. The

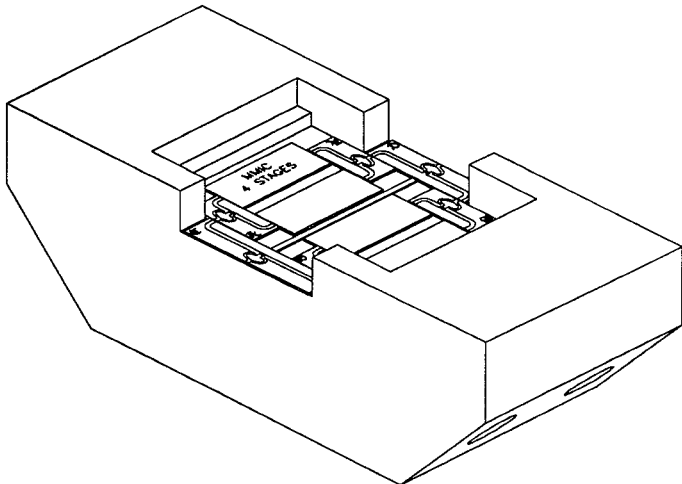


Fig. 3. 47 GHz four-way combined power amplifier.

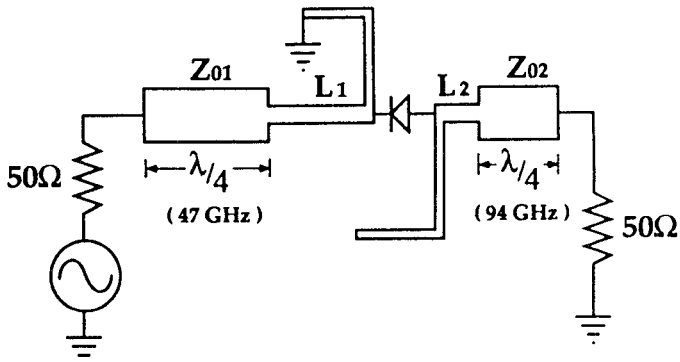


Fig. 4. Circuit schematic of W-band doubler.

breakdown voltage of the diode was estimated to be 20.5 V. The thickness of the active layer was, in turn, determined to be 0.65 μm from the doping concentration and breakdown voltage so as to keep the depletion layer in the active region from penetrating into the substrate at full drive condition. By using the optimized diode doping profile, a zero-biased cut-off frequency higher than 1,100 GHz was achieved.

Fig. 4 is a circuit schematic of the MMIC doubler. A $\lambda/4$ (at 47 GHz) shorted stub at the input side of the diode, which is equivalent to $\lambda/2$ of 94 GHz, is used to create an RF short circuit at 94 GHz to prevent the output power generated by the diode nonlinearity from traveling backward. Similarly, a $\lambda/4$ (at 47 GHz) open stub at the output side of the diode, generates an RF short at 47 GHz and causes the input signal penetrating through the diode to be reflected back. Since the diode is modeled as a voltage-dependent capacitive impedance, inductive source and load terminations are required in order to resonate the diode junction capacitance to obtain maximum efficiency and output power [11] [12]. As shown in the MMIC photograph, a section of transmission line is used as an inductor and a $\lambda/4$ impedance transformer is used to transform $50\ \Omega$ to the optimum diode terminations. Some parameters of the varactor diode, together with the measured results, are given in Table I. Simulated results of a

TABLE I
COMPARISON OF MEASURED AND PREDICTED DIODE PARAMETERS AND DOUBLER PERFORMANCE

Description	Predicted	Measured
Active layer doping	$7 \times 10^{16}\ \text{cm}^{-3}$	
n^+ layer doping	$8 \times 10^{18}\ \text{cm}^{-3}$	
Diameter of Schottky contact	16 μm	
Active layer thickness	0.65 μm	
n^+ layer thickness	2.5 μm	
Series resistance R_s	0.82 Ω	0.87
Zero-biased capacitance (C_{j0})	0.17 pF	0.17 pF
Breakdown Voltage (V_B)	20.5 V	18 V
Efficiency (η) @ 330 mW input	28.1%	19.7%
Output power @ 330 mW input	93 mW	65 mW

94 GHz doubler in LIBRA using the diodes are also presented in Table I. Excellent agreement of the predicted values with the measured results was achieved, and the validity of the analysis was verified.

To achieve usable power at 94 GHz for system applications, a two-way combined doubler using the above MMIC doubler chips was also developed. The hybrid combiners for 94 GHz and dividers for 47 GHz were in-phase Wilkinson-type circuits which were fabricated on 5-mil-thick fused silica substrate.

III. MMIC FABRICATION

The amplifiers were fabricated on epitaxial layers grown by the molecular beam epitaxy (MBE) technique. MBE material was used with an active n layer of $4.5 \times 10^{17}\ \text{cm}^{-3}$ doping concentration and a contact n^+ layer concentration of $3 \times 10^{18}\ \text{cm}^{-3}$. The chips were isolated by the mesa-etching process and a combination of direct-write e-beam and optical lithography was used for defining 0.3 μm gates and fabrication of the circuits. Au-Ge-Ni-Au alloy and Ti-Pt-Au metallizations were used for the ohmic contacts and gates, respectively. Si_3N_4 was used for the MIM capacitor dielectric, and for the chip passivation. The dielectric layer was 2500 \AA thick, providing a capacitance of 220 pF/mm². The chips have via-holes for source grounding. Mesa-resistors in the range of 100 Ω were used as resistive power termination for the on-chip Wilkinson power combiner/divider. Fig. 5 shows the MMIC chip with dimensions of 5.0 \times 2.8 \times 0.09 mm.

The doubler was fabricated on a vapor phase epitaxy (VPE) substrate that had a buried n^+ layer to minimize the diode series resistance [8]. VPE material was used with an active n layer of $7 \times 10^{17}\ \text{cm}^{-3}$ doping concentration and a contact n^+ layer concentration of $8 \times 10^{18}\ \text{cm}^{-3}$. An Au-Ge-Ni-Ag-Au alloy was also used for the ohmic contact, and Ti-Pt-Au metallization for Schottky barrier contacts. Si_3N_4 was used for both the capacitor dielectric layer and chip passivation. Following completion of the circuits through the front side, via-holes were etched in the thinned wafer. Gold was then plated onto the backside and via-holes to a thickness of 10 μm prior to dicing the chips. The diode has a breakdown voltage

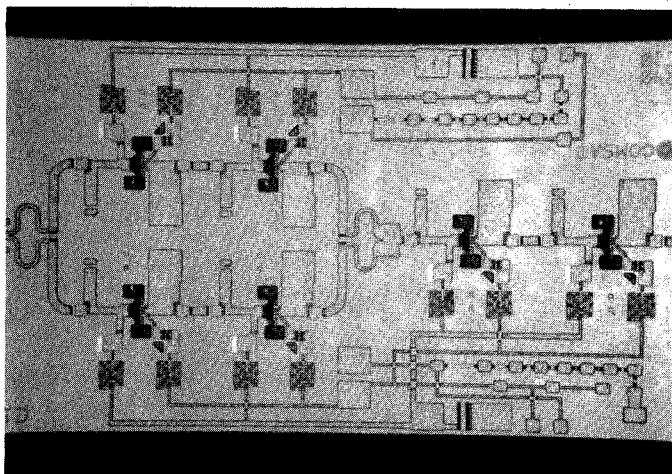


Fig. 5. Microphotograph of 47-GHz GaAs MESFET power MMIC chip (chip size: $5.0 \times 2.8 \times 0.09$ mm).

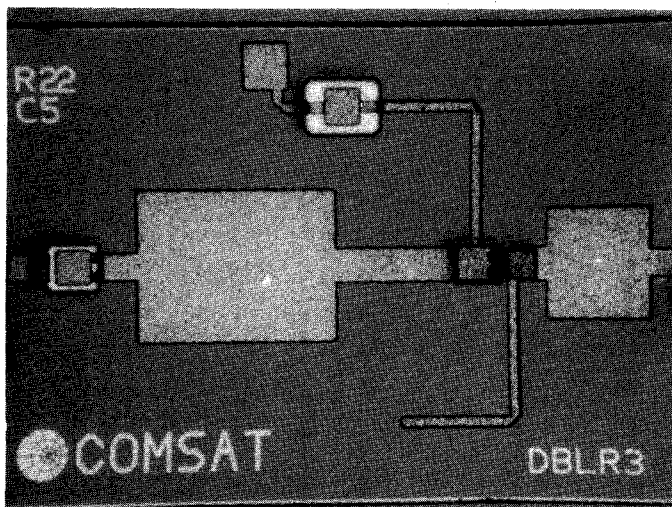


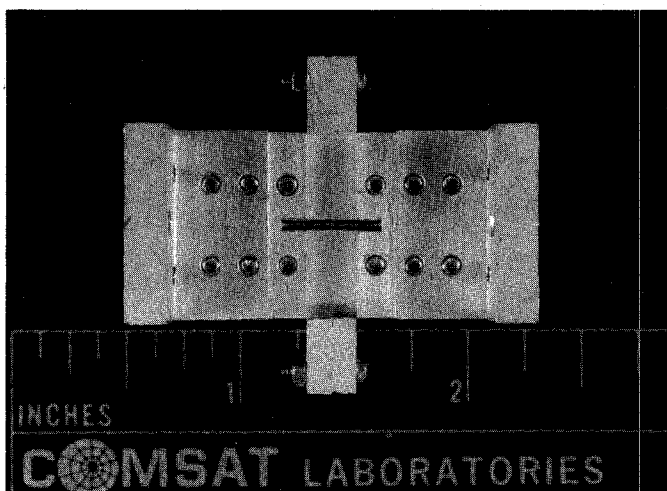
Fig. 6. Microphotograph of 94-GHz GaAs MMIC doubler chip (chip size: $1.5 \times 1.0 \times 0.09$ mm).

greater than 16 V. Fig. 6 shows the MMIC doubler chip with dimensions of $1.5 \times 1.0 \times 0.09$ mm.

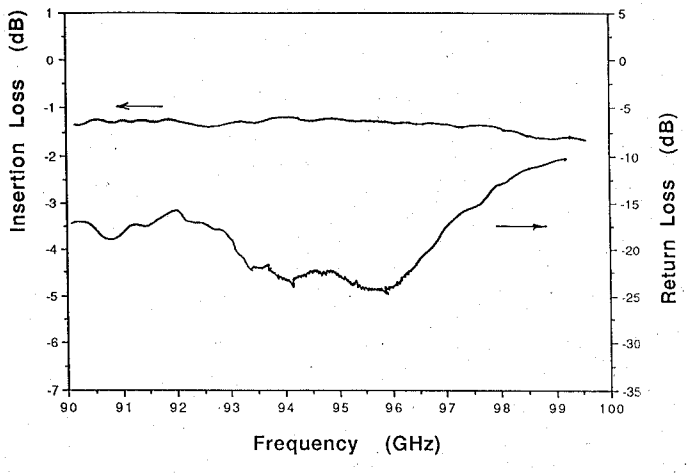
IV. CIRCUIT PERFORMANCE

Waveguide-to-Microstrip Transitions

A high-performance waveguide-to-microstrip transition is essential for accurately evaluating MMIC's at *U*- and *W*-band. A ridged-waveguide transition was selected and developed to provide low RF loss and a rigid structure. Fig. 7(a) shows the *W*-band waveguide-to-microstrip transition housing. A 5-mil-thick fused silica substrate was mounted on transition housing using silver epoxy, and a 10-mil-wide gold ribbon was thermally bonded from the ridge to microstrip line to have a good electrical contact. Fig. 7(b) shows the performance to two transitions measured back-to-back with two 200-mil fused silica $50\ \Omega$ transmission lines. From the frequency 90–97 GHz, the insertion loss and return loss of each transition were typically 0.6 dB and better than 16 dB, respectively. The *U*-band performance of two transitions was also



(a)



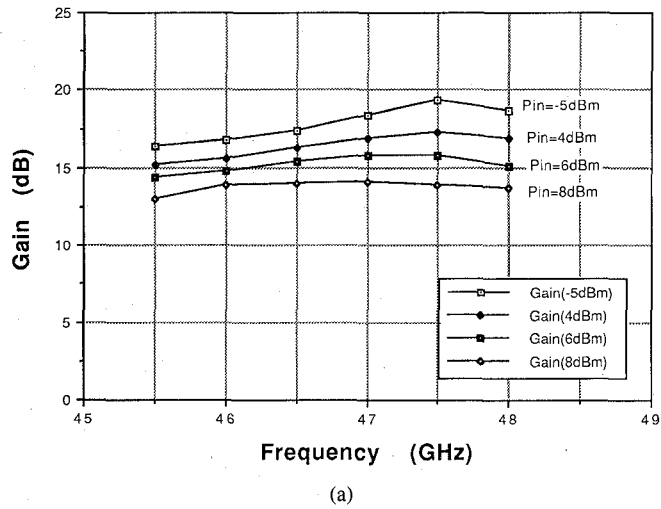
(b)

Fig. 7. *W*-band waveguide-to-microstrip transition. (a) Transition housing assembly. (b) *W*-band performance of two transitions measured back-to-back (with two 200-mil-long $50\ \Omega$ lines on fused silica substrate).

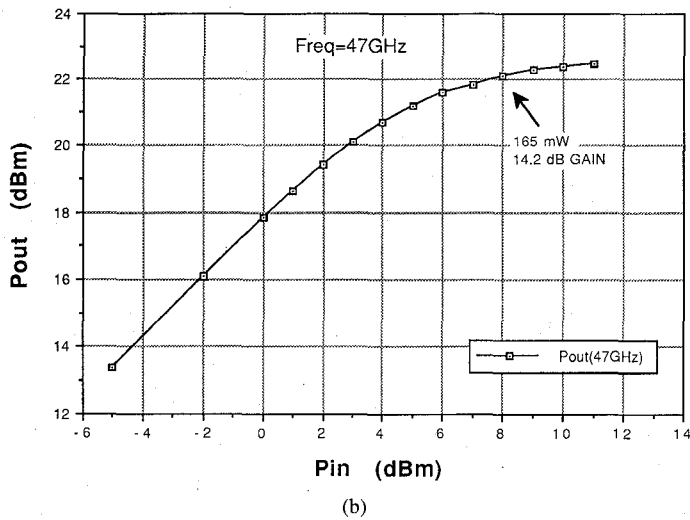
measured back-to-back with 70-mil fused silica $50\ \Omega$ lines. Over the frequency range of 40–48 GHz, the insertion loss was typically 0.25 dB and the return loss was better than 20 dB for each transition. The above ridged waveguide-to-microstrip transitions were used to evaluate the MMIC chips at *U*- and *W*-band.

U-Band Power Amplifier

The MMIC power amplifier chips were tested by mounting in a *U*-band amplifier test fixture, which consisted of a copper center block and a pair of low-loss ridged waveguide-to-microstrip transitions. A four-stage MMIC power amplifier chip was assembled and tested using the *U*-band waveguide test setup. The associated overall gain versus frequency is shown in Fig. 8(a) for four input drive levels, namely, -5, 4, 6 and 8 dBm. The amplifier associated gain is about 14.2 dB across the frequency band from 46.5–47.5 GHz with an output power level of 165 mW. The input and output return losses were better than 15 and 9 dB, respectively, in the same fre-



(a)



(b)

Fig. 8. Measured performance of four-stage GaAs MESFET power amplifier. (a) Power gain versus frequency. (b) Output power versus input power.

quency band. Fig. 8(b) shows the power transfer characteristics of the amplifier at 47 GHz. A saturated power of over 180 mW with 11.2% power added efficiency was also achieved. Stable power amplification was achieved without connecting any off-chip stabilizing R-C elements. This result represents the highest power gain and complexity known from a single MMIC chip at *U*-band.

A four-way combined MMIC power amplifier was also assembled and tested using the above power MMIC chips as shown in Fig. 3. The complete four-way combined power amplifier module assembly with the input and output ridged waveguide-to-microstrip transitions is shown in Fig. 9. The associated power gain versus frequency is shown in Fig. 10(a), namely, -10, 5, 8, and 10 dBm. For this data, the amplifier was biased with $V_{ds} = 4.5$ V and $V_{gs} = 0.75$ V. The amplifier associated gain is about 16.6 dB across the frequency band of 46.5–47.5 GHz with an output power of 460 mW. The output power versus input power of the amplifier is shown in Fig. 10(b) for 47 GHz. A saturated output power of over 0.58 W with 8.6% power added efficiency was also achieved at 47 GHz.

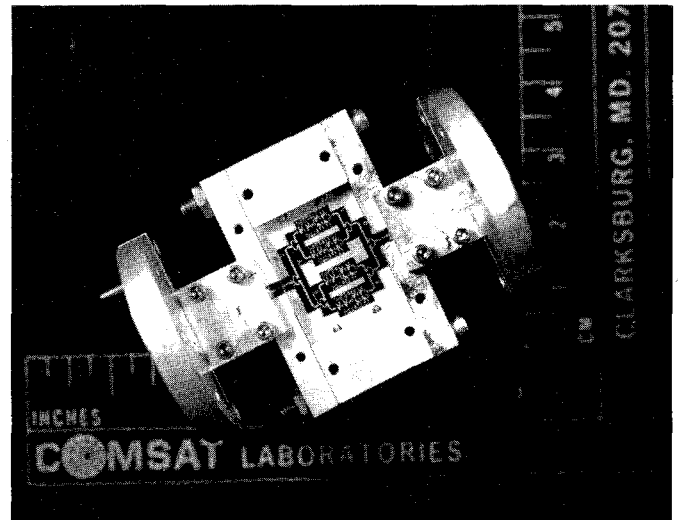
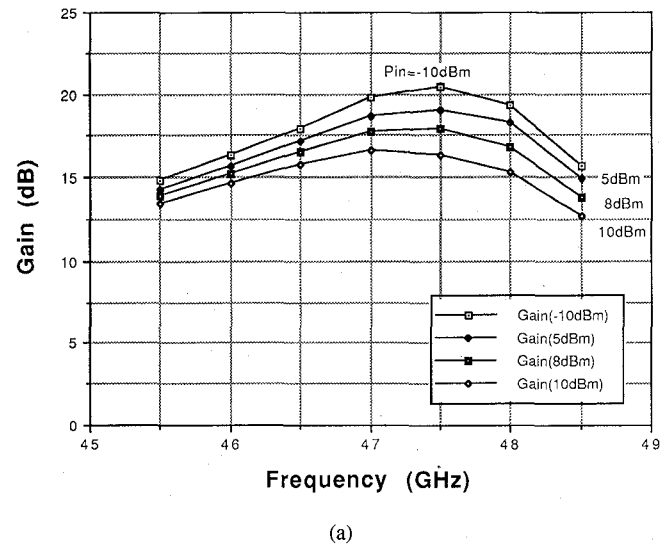
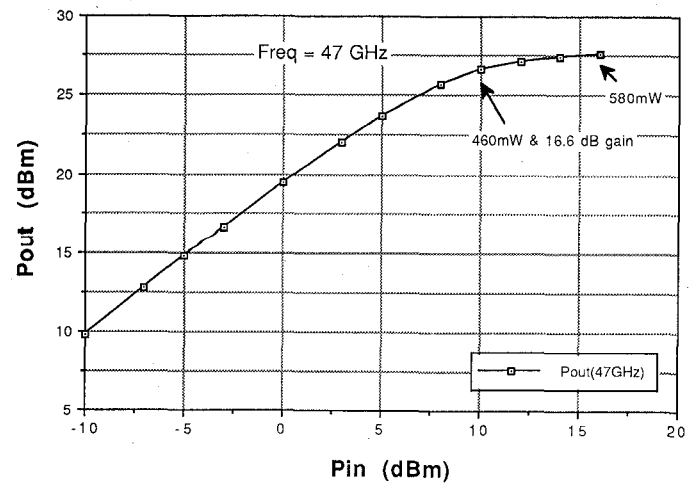


Fig. 9. Complete four-way combined power amplifier module assembly.

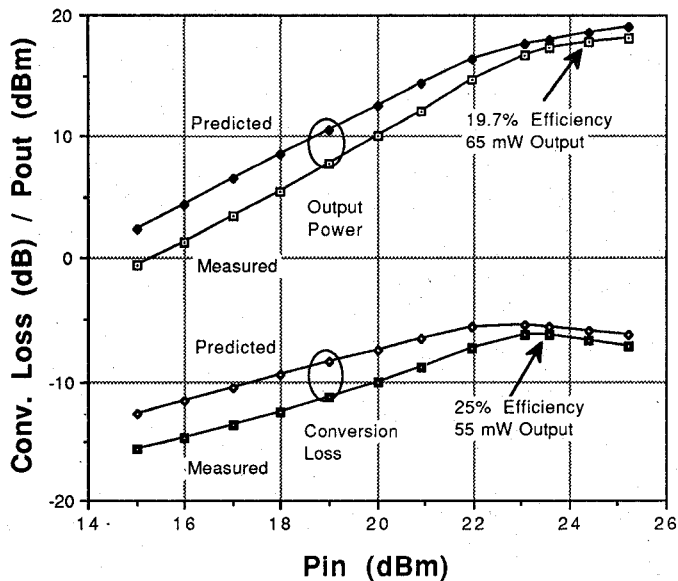


(a)



(b)

Fig. 10. Measured performance of four-way combined power amplifier. (a) Power gain versus frequency. (b) Output power versus input power ($V_{ds} = 4.5$ V, $I_{ds} = 1.4$ A).

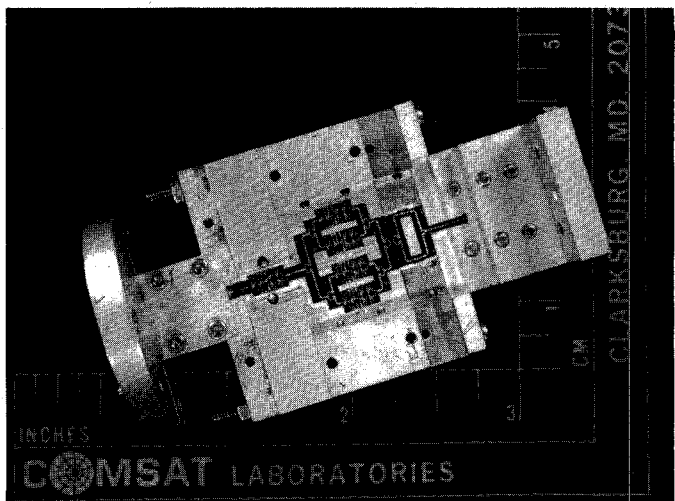
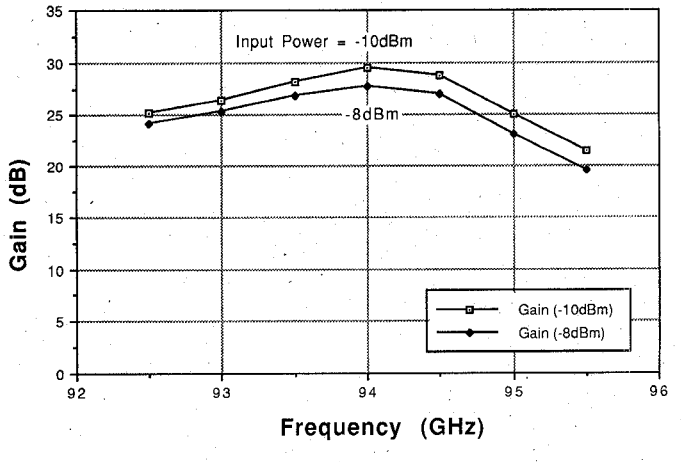
Fig. 11. Performance of *W*-band MMIC doubler.

W-Band Varactor Doubler

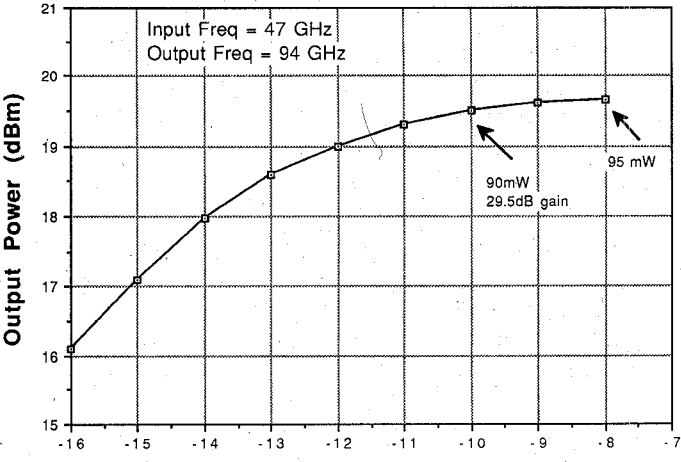
The doubler was RF tested by mounting the chip to a test fixture consisting of a *U*-band and *W*-band output microstrip to ridged waveguide transitions. The measured output power and efficiency with input power from 15–25 dBm are shown in Fig. 11. The reverse bias applied to the varactor diode was 7 V. The doubler exhibited maximum efficiency of 25% (6 dB conversion loss) and output power of 55 mW at input power of 220 mW. Sixty-five mW output power at 94 GHz was obtained at an input level of 330 mW at 47 GHz. These results represent the highest reported power and efficiency using a MMIC doubler at *W*-band. The predicted output power and efficiency using LIBRA and the nonlinear diode model described in a previous section, are also shown in the figure and exhibit very good agreement with the measured results.

W-Band Integrated Power Module

To achieve over 90 mW output power at 94 GHz, an integrated module was also assembled and tested. Fig. 12 shows the complete integrated power module assembly with input (47 GHz) and output (94 GHz) ridged waveguide-to-microstrip transitions. The associated power gain versus frequency is shown in Fig. 13(a), namely, -10 and -8 dBm. For this data, the amplifier was biased with $V_{ds} = 4.5$ V and $V_{gs} = 0.75$ V, and the doubler was biased with $V_d = 7$ V. The total current input of this integrated power module is about 1.76 A. The overall associated gain of the integrated power module is about 27.4 dB across the frequency band from 93.5–94.5 GHz with an output power level of 80 mW. The output power versus input power of the integrated power module is shown in Fig. 13(b). An output power of 90 mW with an overall associated power gain of 29.5 dB was measured at 94 GHz. A saturated output power of over 95 mW was also achieved at the same frequency.

Fig. 12. Complete *W*-band integrated power module assembly.

(a)



(b)

Fig. 13. Measured performance of *W*-band integrated power module. (a) Power gain versus frequency. (b) Output power versus input power.

V. CONCLUSION

A *W*-band integrated power module using *U*-band MMIC MESFET power amplifiers in conjunction with *W*-band MMIC high efficiency varactor doubler has been

designed, fabricated, and tested. Measured results of the complete integrated power module show an output power of 90 mW with an overall associated gain of 29.5 dB at 94 GHz. A saturated power of over 95 mW was also achieved. This is the first successfully developed W-band integrated power module with 95 mW output power at 94 GHz. This integrated power module is suitable as a transmitter source for 94 GHz missile seeker applications.

ACKNOWLEDGMENT

The authors wish to thank J. Bass, A. Cornfield, E. Carlson, R. Dean, S. Huynh, T. Noble, J. Proctor, P. Phelleps, J. Singer, and S. Tadayon for their technical assistance.

REFERENCES

- [1] G. Metze, T. Lee, J. Bass, P. Laux, H. Carlson, and A. Cornfield, "A narrow-channel 0.2 μm gate-length: Double quantum-well pseudomorphic MODFET with high power gain at millimeter-wave frequencies," *IEEE Electron Device Lett.*, vol. 11, pp. 493-495, Nov. 1990.
- [2] R. Majid-Ahy, M. Riaziat, C. Nishimoto, M. Glenn, S. Silverman, S. Weng, Y. Pao, G. Zdziak, S. Bandy, and Z. Tan, "5-100 GHz InP CPW MMIC 7-section distributed amplifier," *IEEE Microwave & Millimeter-Wave Monolithic Circuit Symp. Tech. Dig.*, pp. 31-34, May 1990.
- [3] P. M. Smith, M. Y. Kao, P. Ho, P. C. Chao, K. H. G. Duh, A. A. Jabra, R. P. Smith, and J. M. Ballingall, "A 0.15 μm gate length pseudomorphic HEMT," *IEEE-MTT-S Symp. Dig.*, pp. 983-986, June 1989.
- [4] T. Ho, K. Pande, F. Phelleps, J. Singer, P. Rice, J. Adair, and M. Ghahremani, "U-band monolithic millimeter-wave GaAs MESFET power amplifier," *IEE Electronics Lett.*, vol. 28, no. 23, pp. 2182-2183, Nov. 1992.
- [5] T. Ho, F. Phelleps, G. Hegazi, K. Pande, and H. Huang, "35 GHz monolithic GaAs FET power amplifiers, in *1990 IEEE-MilCom, Conf. Proc.*, pp. 184-186, Oct. 1990.
- [6] G. Hegazi, H. Hung, F. Phelleps, A. Cornfield, T. Smith, J. Allison, and H. Huang, "V-Band monolithic power MESFET amplifiers," *IEEE-MTT-S Symp. Dig.*, pp. 409-412, May 1988.
- [7] J. A. Calviello, J. L. Wallace, and P. R. Bie, "High performance quasi-planar varactors for millimeter waves," *IEEE Trans. Electron Devices*, vol. ED-21, pp. 624-630, Oct. 1974.
- [8] J. A. Calviello, "Advanced devices and components for the millimeter and sub-millimeter systems," *IEEE Trans. Electron Devices*, vol. ED-26, pp. 1273-1281, Sept. 1979.
- [9] S. M. Sze, *High Speed Semiconductor Device*. New York: Wiley-Interscience, 1990.
- [10] T. C. Leonard, "Prediction of power and efficiency of frequency doublers using varactors exhibiting general nonlinearity," *Proc. IEEE*, pp. 1135-1139, Aug. 1963.
- [11] P. Penfield, Jr. and R. P. Rafuse, *Varactor Applications*. Cambridge, MA: MIT Press, 1962.
- [12] E. Bava, G. Paolo, A. Godone, and G. Rietto, "Analysis of Schottky barrier millimetric varactor doublers," *IEEE Trans. Microwave Theory Techniques*, vol. MTT-29, pp. 1145-1149, Nov. 1981.
- [13] G. Hegazi, A. Ezzeddine, F. Phelleps, P. McNally, and K. Pande, "W-band monolithic frequency doubler using vertical GaAs varactor diodes with n^+ buried layer," *IEE Electronics Lett.*, vol. 27, pp. 213-214, Jan. 1991.

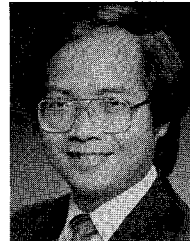


Thomas C. Ho (S'75-M'76-SM'90) received the B.S.E.E. degree from Chung Cheng Institute of Technology, Taiwan, in 1970, the M.S.E.E. degree from the University of California, Los Angeles, in 1975, and the Ph.D. degree from Cornell University in 1984.

Prior to 1988, he was with Chung Shan Institute of Science and Technology, Taiwan. He was also a part-time Professor of Electrical Engineering, National Taiwan University. He is currently Manager of the Microwave Components Department

of the Microwave Electronics Division at COMSAT Laboratories, Clarksburg, MD, where he is involved in the research and development of monolithic components and subsystems. His present responsibilities include the design, module integration, testing, and production of high reliability microwave and millimeter-wave hardware. He is also Program Manager on several contracts from defense systems companies. He has more than 20 years experience in the microwave field.

Dr. Ho was awarded the Chinese Government's highest honor, the Yun-Wei Medal, for his achievements in microwave components and subsystems development. He is the author of over 30 papers in the area of microwave and millimeter-wave integrated circuits and systems. He is a member of Eta Kappa Nu and Tau Beta Pi.



Seng-Woon Chen was born in Keelung, Taiwan, in 1961. He received the B.S. degree from National Taiwan University, Taipei, Taiwan, in 1982, and the M.S. and Ph.D. degrees from the University of Maryland, College Park, in 1988 and 1990, respectively, all in electrical engineering.

From 1982 to 1984, he served in the Army Military Police Headquarters as a Second Lieutenant Technical Staff. Beginning in 1984, he spent two years as a member of the technical staff in Microelectronics Technology Inc., Hsin-Chu, Taiwan, where he designed K-band MESFET dielectric resonator stabilized oscillators and phase-locked oscillators for short haul digital microwave radios. While at the University of Maryland, he held a Graduate Research Assistantship in Microwave Laboratories and conducted research on the analysis and modeling of dielectric loaded waveguides, resonators, periodic structures, and filters. In 1990, he joined COMSAT Systems Divisions, Clarksburg, MD, where he was engaged in systems analysis and design of earth station for satellite communications. Presently, he is with COMSAT Laboratories, where his research activities have been focused on design and modeling of monolithic microwave and millimeter-wave integrated circuits (MIMIC'S).



Krishna Pande (F'90) received the Ph.D. degree in solid-state physics from the Indian Institute of Technology, in 1973.

Prior to 1988, he was Director at Unisys Semiconductor Operations, a Manager at Bendix Aerospace Technology Center, Assistant Professor at Rutgers University, and Research Associate at Rensselaer Polytechnic Institute. He has been Program Manager on a number of research and development contracts in the area of GaAs components and subsystems from DoD agencies and defense systems companies. Currently, he is Executive Director of the Microwave Electronics Division at COMSAT. He has made significant contributions in the area of III-V devices, circuits, and materials technology, having published over 75 research papers. He also holds three patents.

Dr. Pande is a member of the American Physical Society Electromagnetic Academy, and the New York Academy of Sciences. He was Vice Chairman of the IEEE Washington chapter for EDS and served on the ERC Technology Advisory Committee for NSF. He has been included in a number of biographical references including *Who's Who in Frontiers of Science and Technology*, *Who's Who in Electromagnetic Academy*, *Who's Who in Technology Today*, *Who's Who in America*, etc. He has delivered invited talks and chaired sessions at many international conferences.



Paul D. Rice received the B.S.E.E. degree from the University of Florida, in 1966 and the M.S.E.E. degree from Southern Methodist University, in 1969. He has completed graduate courses at Southern Methodist University, Texas Christian University, and the University of South Florida.

Currently, he is a Principal Engineer with Hercules Defense Electronics Systems (HDES). He has 27 years experience in the design, development, testing, and analysis of various microwave, mm-wave, and IF/analog circuits and subsystems. These subsystems include MMW seekers, electronic warfare, radar simulators, automatic network analyzers, ATE, and operational level equipment. He is presently responsible for several research and development projects applying GaAs MMIC's to MMW seeker Transceivers and is the HDES Phase II MIMIC brassboard Program Manager.